Simple endotoxin detection using polymyxin B-gated nanoparticles

Ismael Otri,[a],[b] Sameh El Sayed,[a],[b] Serena Medaglia, [a],[b] Ramón Martínez-Máñez,[a],[b],[c]* Elena Aznar,[a],[b]* and Félix Sancenón[a],[b],[c]

Abstract: A nanodevice based on mesoporous silica nanoparticles with rhodamine B in the pore framework, functionalised with carboxylates on the outer surface and capped with the cationic polymyxin B peptide was used to selectively detect endotoxin in aqueous solution with a limit of detection in the picomolar range.

Endotoxin, also known as lipopolysaccharide (LPS), is one of the major components of the outer membrane of gram-negative bacteria.[1] Endotoxin is composed of variable polysaccharide chains attached to a phosphorylated glucosamine disaccharide decorated with multiple fatty acids.[2] Gram-negative bacteria, after their death, release this highly stable molecule to the surrounding environment.[3,4] Exposure to endotoxin contaminated environments (water or air) can lead to the development of several health problems such as pulmonary inflammation, respiratory difficulties, asthma, diarrhea, vomiting and fever.[5]

Several methods for the detection of endotoxin in environmental samples have been developed.[6] Among them, the Limulus amebocyte lysate (LAL) test is one of the most widely used for endotoxin quantification. However, this test suffers several drawbacks such as false positive readings (by pectic polysaccharides and β-(1,3)-D-glucan),[7-9] is highly affected by temperature and pH changes, requires sample preparation procedures, and the use of controlled experimental conditions.[10] Taking into account the above mentioned facts, the development of reliable, accurate and easy to use sensing methods for endotoxin detection is an issue of interest. In this scenario, optical chemosensors,[11-14] gold nanoparticles,[15] iron oxide-gold nanoflowers[16] or graphene quantum dots[17] have been explored as alternatives to classical methods for endotoxin sensing.[18]

From another viewpoint, there is an increasing interest in the design of gated porous nanomaterials for sensing and recognition protocols.[19,20] These nanomaterials are composed by a porous inorganic support (usually mesoporous silica) designed in such a way that dye release from the pores is selectively observed only when the target analyte is present. To achieve this functionality, the external surface of the loaded inorganic support is functionalized with molecular or supramolecular entities that inhibit dye delivery. However, in the presence of the analyte, the pores open due to the interaction of the analyte with the capping ensemble leading to cargo release.[21-26] One of the advantages of these solids is the potential existence of amplification features as few analyte molecules may trigger gate opening, and induce the release of a high amount of entrapped dye molecules.

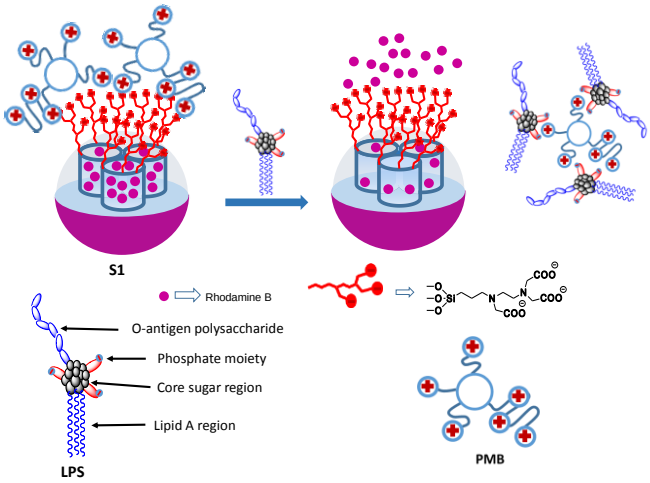

Scheme 1. Representation of the performance of the capped solid **S1** able to detect the presence of endotoxin.

Given our interest in exploring the potential use of gated nanomaterials in sensing protocols, we report herein a new nanodevice based on mesoporous silica nanoparticles (MSNs) functionalized with carboxylate moieties and capped with the cationic peptide polymyxin B for the selective and sensitive detection of endotoxin. The proposed recognition paradigm is depicted in Scheme 1. MSNs are selected as inorganic porous support. The pores of the nanomaterial are loaded with the rhodamine B fluorophore (as reporter) and the outer surface of the rhodamine B-containing nanoparticles is functionalized with carboxylates and finally capped with polymyxin B. Polymyxin B contains two separated lipophilic and hydrophilic domains. The lipophilic domain of polymyxin B is known to shows a very strong affinity for the disaccharide decorated with fatty acids of the endotoxin molecule. In fact, polymyxin B is used in the treatment of gram-negative bacterial infections.[27] In our system, a selective displacement of polymyxin B and rhodamine B release in the presence of endotoxin is expected to occur. To our knowledge, this is the first polymyxin B-capped hybrid nanomaterial used for the fluorogenic detection of endotoxin.

Mesoporous silica nanoparticles (MSNs) were synthesized according to a described procedure which uses the structure-directing agent *n*-cetyltrimethylammonium bromide (CTAB) and tetraethylorthosilicate (TEOS) as silica source.[28,29] The pore framework of the material was loaded with the fluorescent molecule rhodamine B. In a subsequent step, the external surface was functionalized with *n*-[(3-trimethoxysilyl)propyl]

[a] I. Otri, Dr. S. El Sayed, S. Medaglia, Prof. R. Martínez-Máñez,* Dr. E. Aznar,* Dr. F. Sancenón,
Instituto Interuniversitario de Investigación de Reconocimiento Molecular y Desarrollo Tecnológico (IDM), Universitat Politècnica de València, Universitat de València. Universitat Politècnica de València, Camino de Vera s/n, 46022, Valencia, Spain. E-mail: rmaez@qim.upv.es, elazgi@upvnet.upv.es

[b] I. Otri, Dr. S. El Sayed, S. Medaglia, Prof. R. Martínez-Máñez,* Dr. E. Aznar,* Dr. F. Sancenón,
CIBER de Bioingeniería, Biomateriales y Nanomedicina (CIBER-BBN), Spain.

[c] Dr. F. Sancenón, Prof. R. Martínez-Máñez,*
Departamento de Química, Universitat Politècnica de Valencia, Camino de Vera s/n, 46022, Valencia, Spain.

Supporting information for this article is given via a link at the end of the document.

ethylene diamine triacetic acid. Then, pores of the nanoparticles were capped, through electrostatic interactions, upon addition of the polymyxin B cationic peptide. Finally, nanoparticles were washed with PBS to remove the rhodamine B adsorbed in the outer surface to obtain the final material (solid **S1** in Scheme 1).

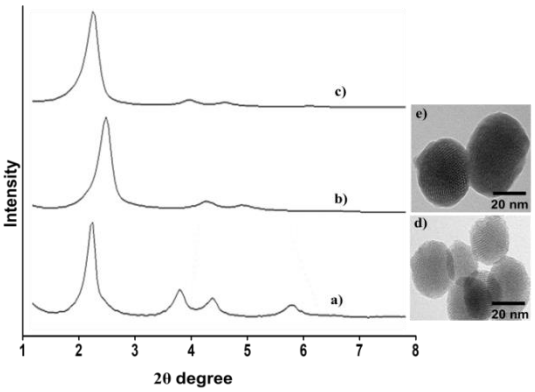

Figure 1. Left: PXRD patterns of (a) mesostructured silica nanoparticles (as-made MSNs), (b) calcined mesoporous nanoparticles and (c) solid **S1**. Right: Representative transmission electron microscopy images of (d) calcined MSNs and (e) solid **S1**.

The starting MSNs (as synthesized and calcined) and **S1** solid were full characterized. Transmission electron microscopy (TEM) and powder X-ray diffraction (PXRD) studies of the nanoparticles confirmed the mesoporous structure of the materials (Figure 1). N_2 adsorption-desorption isotherms of calcined MSNs showed a type IV curve. From BET and BJH models, a specific surface area of 1069 $m^2 g^{-1}$ and an average pore diameter of 2.66 nm was estimated for the starting MSNs, whereas the specific surface area decreased to 279 $m^2 g^{-1}$ for **S1** (Table 1). Moreover, elemental and thermogravimetric analysis were used to determine the amount of rhodamine B, tricarboxylate derivative, and polymyxin B in solid **S1** (Table 2).

Table 1. Main structural features of calcined MSNs and **S1** nanoparticles determined by PXRD, TEM and N_2 isotherm adsorption-desorption measurements.

Sample	Particle diameter[a] (nm)	Surface area, S_{BET} ($m^2 g^{-1}$)	Pore Volume[b] ($cm^3 g^{-1}$)	Pore size[c] (nm)
MSNs	110	1011	0.86	2.66
S1	122	279	0.14	-

[a] Measured by TEM.
[b] Pore volume (from BJH for $P/P_0 < 0.6$, associated to mesopores).
[c] Pore size (from BJH model for $P/P_0 < 0.6$).

Table 2. Content (α) of rhodamine B, anchored tricarboxylate and polymyxin B in solid **S1**.

Solid	$\alpha_{rhodamine\ B}$ [mmol g^{-1} SiO_2]	$\alpha_{tricarboxylate}$ [mmol g^{-1} SiO_2]	$\alpha_{polymyxin\ B}$ [mmol g^{-1} SiO_2]
S1	0.073	0.035	0.089

After characterization of the prepared nanoparticles, the sensing behavior of **S1** in the presence of endotoxin (from *E. coli*) was tested. Two portions of solid **S1** (0.5 mg) were suspended in PBS at pH 7.4 (1 mL). Then, endotoxin (1000 μg mL^{-1}) was added to one batch while the volume of the other portion was adjusted with endotoxin-free PBS (blank). At certain scheduled times aliquots of both experiments were separated and filtered. The emission of the rhodamine B released to the solution was measured at 571 nm (λ_{ex} = 555 nm). The obtained results are shown in Figure 2. As it could be seen, when endotoxin is absent, nearly a zero release of rhodamine B was observed according to an efficient pore closure promoted by the strong electrostatic interaction between the grafted tricarboxylate moieties and the cationic polymyxin B. As a clear contrast, in the presence of endotoxin, a high increase in rhodamine B release was monitored. A 90% of the total released dye was achieved only after 30 min. Thus, the sensing mechanism can be explained in terms of the uncapping event. When the capped nanoparticles are in the presence of endotoxin, this molecule induces pore unblocking and subsequent rhodamine B release due to the formation of a complex between polymyxin and the target endotoxin, which is stronger than the interaction with the solid surface.

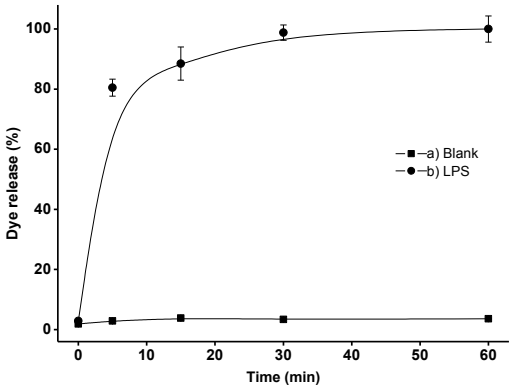

Figure 2. Rhodamine B release profile obtained from suspensions of **S1** when endotoxin is absent and present (1000 μg mL^{-1}) at 25°C in PBS (pH 7.4).

In a second step, cargo release from **S1** upon addition of increasing concentrations of endotoxin was studied. For this purpose, and following a similar procedure to that described above, rhodamine B release from **S1** at 30 min and using different amounts of endotoxin was registered. Figure 3 shows the obtained calibration curve. As it can be observed, there is a direct correlation between the endotoxin concentration and the amount of rhodamine B delivered from **S1**. From the obtained data a limit of detection (LOD) for endotoxin of 100 pg mL^{-1} was determined. This LOD is similar to those reported for other hybrid sensors based on the use of gold nanoparticles.[30-32]

Besides, **S1** nanoparticles yielded a remarkable fluorescence response in the presence of endotoxin after 10 min, being much faster than the standard LAL method (ca. 60 min) used for the detection of this toxin. In addition, **S1** nanoparticles showed a high stability at 25°C and did not require a special storage or severe temperature requirements. As mentioned above, one interesting feature of gated materials applied in detection protocols is the possibility to observe signal amplification due to a remarkable delivery of the entrapped reporter in the presence of only few analyte molecules. In particular, using **S1**, one LPS molecule (at 1.0×10^{-5} mol dm^{-3}

concentration) induced the release of ca. 200 molecules of rhodamine B.

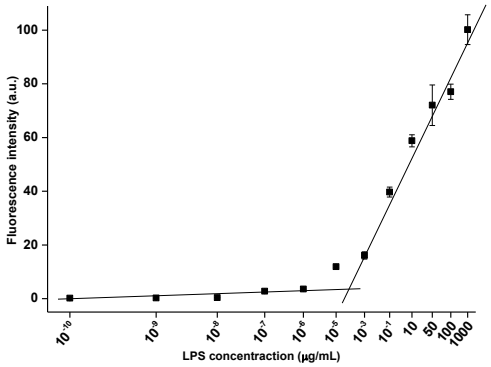

Figure 3. Calibration curve of rhodamine B released from **S1** nanoparticles (PBS, pH 7.4) in response to different quantities of endotoxin after 30 min.

Moreover, the selectivity of solid **S1** toward endotoxin was studied by analyzing cargo release from the nanoparticles in the presence of common interfering agents such as arabinogalactan (AG), β-(1,3)-D-glucan, pectin, EDTA, glucose, GTP, DNA, RNA and dust (endotoxin free). Figure 4 shows the response at 30 min of **S1** nanoparticles suspended in PBS (pH 7.4) or in tap water in the presence of endotoxin (from *E. coli* and *R. sphaeroides*) and the selected interfering agents (at 50 μg mL^{-1}). As could be seen, only endotoxin was able to induce pore opening and rhodamine B release. This was a remarkable result because the presence of pectin and β-(1,3)-D-glucan usually results in false positives when the LAL method is used.[33] Besides, the same selective response to endotoxin was observed in the presence of a mixture of endotoxin and the selected interfering compounds (see Supporting Information).

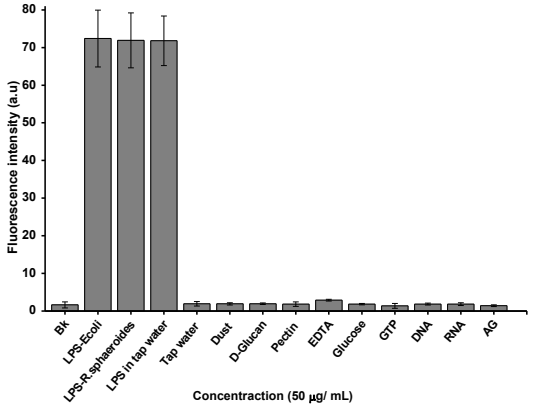

Figure 4. Response of **S1** to endotoxin and selected interfering agents (50 μg mL^{-1}).

In addition, the controlled release behavior of **S1** nanoparticles at different pH was also tested. The pH range in which **S1** nanoparticles could be used to effectively detect endotoxin is 4.0-8.5 (see Supporting Information). As expected, at pH 2, tricarboxylate groups on the external surface of the nanoparticles become fully protonated and negligible interactions with polymyxin B were present. As a consequence a substantial delivery of rhodamine B was observed when the material is exposed to acidic pH.

Table 3. Endotoxin determination in different samples of spiked tap water samples using **S1** nanoparticles.

Sample	Spiked endotoxin (μg)	Determined endotoxin (μg)	Recovery (%)
1	500	517	96.7
2	50	52.3	95.6
3	10	9.5	94.8

Finally, we centered our attention in the possible application of **S1** as an endotoxin probe. In the routine practice, the LAL assay is the most widely used endotoxin detection method. However, it requires a controlled workplace to proceed with a complex sample and it is also a time consuming assay. Development of simple alternative methodologies which would give a faster response could be pivotal in many sectors such as health, environment and food industry. Following these ideas, the applicability of **S1** nanoparticles for endotoxin detection in a more realistic environment such as tap water was studied. Water is one of the most common media that bacteria use to grow and spread to other systems. Aliquots of 450 μL of water were spiked with known amounts of endotoxin (500, 50 and 10 μg). The different samples were mixed with 500 μg of **S1**. Then, rhodamine B release at 30 min was monitored and the corresponding endotoxin concentration was calculated by standard addition. The obtained results are shown in Table 3. As it could be seen, the gated nanomaterial was able to sense the presence of endotoxin in tap water with recoveries in the 95-97% range, which demonstrates the potential applicability of solid **S1** as an effective probe to detect endotoxin in realistic environments.

In summary, we have prepared a new nanomaterial using mesoporous silica nanoparticles as support, rhodamine B as reporter and the cationic peptide polymyxin B as gating mechanism. After characterization, the sensing behavior of the prepared hybrid material against endotoxin was studied. The selective strong coordination, through electrostatic interactions, between endotoxin and the capping polymyxin B induced pore unblocking and the subsequent rhodamine B release. The obtained response was highly selective to endotoxin and other interfering agents such as arabinogalactan, β-(1,3)-D-glucan, pectin, EDTA, glucose, GTP and dust were unable to induce pore opening. Besides, a limit of detection for endotoxin as low as 100 pg mL^{-1} was determined. The probe is stable and allow detection of endotoxin in the 4.0-8.5 pH range. Moreover, the capped nanoparticles were used to detect endotoxin in spiked tap water and obtained high recovery rates. The reported results suggest that polymyxin B-gated nanoparticles could be the basis for the development of an easy-to-use kit to detect endotoxin in contaminated environmental samples.

Acknowledgements

The authors thank the Spanish Government (MAT2015 64139-C4-1-R) and the Generalitat Valenciana (PROMETEO2018/024)

for their support. I.O. thanks to Erasmus Mundus Programme, Action 2, Lot 1, Syria his predoctoral fellowship. S.S is grateful to Spanish Ministerio de Economia y Competitividad for his Juan de la Cierva contract (FJCI-2015-27201).

Keywords: Endotoxin • Polymyxin B • mesoporous silica nanoparticles • gated materials • fluorogenic detection

[1] R. J. Ulevitch, P. S. Tobias, *Curr. Opin. Immunol.* **1994**, *6*, 125-130.
[2] L. S. Young, W. J. Martin, R. D. Meyer, R. J. Weinstein, E. T. Anderson, *Ann. Intern. Med.* **1977**, *86*, 456-471.
[3] M. Mueller, B. Lindner, S. Kusumoto, K. Fukase, A. B. Schromm, U. Seydel, *J. Biol. Chem.* **2004**, *279*, 26307-26313.
[4] J. Bhattacharyya, S. Biswas, A. G. Datta, *Curr. Med. Chem.* **2004**, *11*, 359-368.
[5] C. Braun-Fahrlander, J. Riedler, U. Herz, W. Eder, M. Waser, L. Grize, S. Maishch, D. Carr, F. Gerlach, A. Bufe, R. P. Lauener, R. Schierl, H. Renz, D. Nowak, E. V. Mutius, *New Engl. J. Med.* **2002**, *347*, 869-877.
[6] M. T. Madigan, J. M. Martinko, J. Parker, T. D. Brock, Brock biology of microorganisms, **2000**, 9th ed. *Upper Saddle River,* NJ: Prentice Hall, pp. 793-794.
[7] S. J. Reynolds, D. K. Milton, D. Heederik, P. S. Thorne, K. J. Donham, E. A. Croteau, K. M. Kelly, J. Douwes, D. Lewis, M. Whitmer, I. Connaughton, S. Koch, P. Malmberg, B. M. Larsson, J. Deddens, A. Saraf, L. Larsson, *J. Environ. Monit.* **2005**, *7*, 1371-1377.
[8] M. Peters, M. Kauth, J. Schwarze, C. Korner-Rettberg, J. Riedler, D. Nowak, C. Braun-Fahrlander, E. V. Mutius, A. Bufe, O. Holst, *Thorax* **2006**, *61*, 134-139.
[9] M. Peters, P. Fritz, A. Bufe, *Innate Immun.* **2012**, *18*, 694-699.
[10] F. R. Lourenço, T. D. S. Botelho, T. D. J. A. Pinto, *PDA J. Pharm. Sci. Tech.* **2012**, *66*, 542-546.
[11] S. Voss, R. Fischer, G. Jung, K. H. Wiesmüller, R. J. Brock, *J. Am. Chem. Soc*. **2007**, *129*, 554-561.
[12] J. Wu, A. Zawistowski, M. Ehrmann, T. Yi, C. J. Schmuck, *J. Am. Chem. Soc*. **2011**, *133*, 9720-9723.
[13] L. Zeng, J. Wu, Q. Dai, W. Liu, P. Wang, C.-S. Lee, *Org. Lett.*, **2010**, *12*, 4014-4017.
[14] M. Lan, J. Wu, W. Liu, W. Zhang, J. Ge, H. Zhang, J. Sun, W. Zhao, P. Wang, *J. Am. Chem. Soc.* **2012**, **134**, 6685−6694.
[15] J. Sun, J. Ge, W. Liu, X. Wang, Z. Fan, W. Zhao, H. Zhang, P. Wang, S. T. Lee, *Nano Res.* **2012**, *5*, 486-493.
[16] P. Prasad, S. Sachan, S. Suman, G. Swayambhu, S. Gupta, *Langmuir* **2018**, *34*, 7396-7403.
[17] B. Jurado-Sánchez, M. Pacheco, J. Rojo, A. Escarpa, *Angew. Chem. Int. Ed.* **2017**, *56*, 6957-6961.
[18] G. Ahn, S. S. Sekhon, Y. -E. Jeon, M. -S. Kim, K. Won, Y. -H. Kim, J. -Y. Ahn, *Toxicol. Environ. Health. Sci*. **2017**, *9*, 259-268.
[19] F. Sancenón, L. Pascual, M. Oroval, E. Aznar, R. Martínez-Máñez, *ChemistryOpen* **2015**, *4*, 418-437.
[20] E. Aznar, M. Oroval, L. Pascual, J. R. Murguía, R. Martínez-Máñez, F. Sancenón, *Chem. Rev.* **2016**, *116*, 561-718.
[21] S. El Sayed, C. Giménez, E. Aznar, R. Martínez-Máñez, F. Sancenón, M. Licchelli, *Org. Biomol. Chem*. **2015**, *13*, 1017-1021.
[22] Y. L. Choi, J. Jaworski, M. L. Seo, S. J. Lee, J. H. Jung, *J. Mater. Chem.* **2011**, *21*, 7882-7885.
[23] Ll. Pascual, S. El Sayed, R. Martínez-Máñez, A. M. Costero, S. Gil, P. Gaviña, F. Sancenón, *Org. Lett*. **2016**, *18*, 5548-5551.
[24] V. C. Özalp, D. Çam, F. J. Hernandez, L. I. Hernandez, T. Schäferd, H. A. Öktem, *Analyst* **2016**, *141*, 2595-2599.
[25] A. Ribes, S. Santiago-Felipe, A. Aviñó, V. Candela-Noguera, R. Eritja, F. Sancenón, R. Martínez-Máñez, E. Aznar, *Sens. Actuators B Chem*. **2018**, *277*, 598-603.
[26] A. Ribes, E. Pérez-Xifré, E. Aznar, F. Sancenón, T. Pardo, L. F. Marsal, R. Martínez-Máñez, *Sci. Rep.* **2016**, *6*, 38649.
[27] D. Ferrari, C. Pizzirani, E. Adinolfi, S. Forchap, B. Sitta, L. Turchet, S. Falzoni, M. Minelli, R. Baricordi, F. Di Virgilio, *J. Immunol.* **2004**, *173*, 4652-4660.
[28] L. Mondragón, N. Mas, V. Ferragud, C. de la Torre, A. Agostini, R. Martínez-Máñez, F. Sancenón, P. Amorós, E. Pérez-Payá, M. Orzáez, *Chem. Eur. J.* **2014**, *20*, 5271-5281.
[29] I. Candel, E. Aznar, L. Mondragón, C. de la Torre, R. Martínez-Máñez, F. Sancenón, M. D. Marcos, P. Amorós, C. Guillem, E. Pérez-Payá, A. Costero, S. Gil, M. Parra, *Nanoscale* **2012**, *4*, 7237-7245.
[30] J. Sun, J. Ge, W. Liu, X. Lung, Z. Fan, W. Zhao, H. Zhang, P. Wang, S. T. Lee, *Nano Res.* **2012**, *5*, 486-493.
[31] Y. Wang, D. Zhang, W. Liu, X. Zhang, S. Yu, T. Liu, W. Zhang, W. Zhu, J. Wang, *Biosens. Bioelectron.* **2014**, *55*, 242-248.
[32] W. Su, M. Cho, J. D. Nam, W. S. Choe, Y. K. Lee, *Electroanalysis* **2013**, *25*, 380-386.
[33] K. Brandenburg, J. Howe, T. Gutsman, P. Garidel, *Curr. Med. Chem.* **2009**, *16*, 2653-2660.